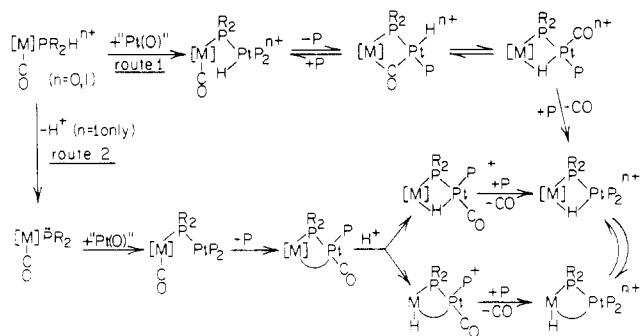
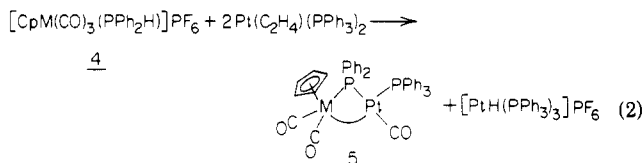


Scheme I. Generalized Reaction Pathways for Pt-Assisted CO Loss and the Formation of μ -Phosphido μ -Hydrido MPt Bimetallic Complexes from the Reactions of (Secondary phosphine)metal Carbonyl Complexes $[M](CO)(PR_2H)^{n+}$ with Pt(O) Complexes^a

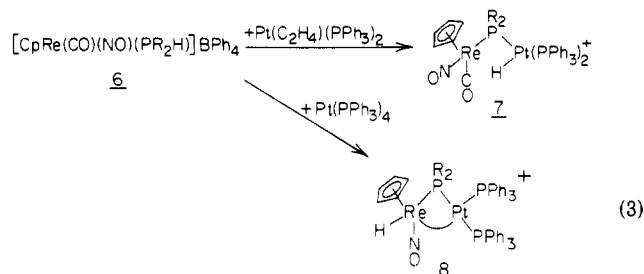


^aRoute 1 involves initial oxidative addition of the P-H bond across Pt(0). Route 2 involves deprotonation of the secondary phosphine to give the phosphido $[M](CO)PR_2$ followed by phosphido substitution of a ligand from the Pt(0) compound as the initial steps of bimetallic complex formation. These reaction pathways have been established from previous studies¹⁻⁴ of a range of phosphido-hydrido-MPt systems. It should be noted that very few of the proposed intermediates have been observed in the current study with the secondary phosphine complexes 9-12. However, the structures, relative distributions, and interconversions of the initially formed MPt products are consistent with the two reaction routes outlined in the scheme.

sitive to the acidity of the P-H bond.² Thus, substitution of a carbonyl ligand by a donor phosphine (e.g. to give $M(CO)_4(PR_3)(PR_2H)$) or replacement of PPh_2H with PCy_2H in $M(CO)_5(PR_2H)$ results in a less acidic P-H bond and markedly retards the oxidative-addition step.¹ In contrast, the P-H bond in cationic secondary phosphine complexes may be more acidic, which leads to an increased reactivity and the observation of a second reaction pathway (Scheme I, route 2). One such example is the complex $[CpM(CO)_3(PPh_2H)]PF_6$ (4; $M = Mo, W$), which reacts almost exclusively via route 2 to give initially the neutral complex $Cp(OC)_2M(\mu-PPh_2)Pt(CO)(PPh_3)$ (5; eq 2).³



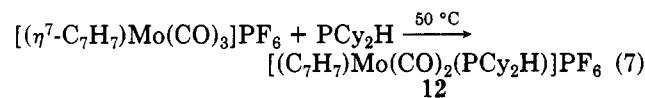
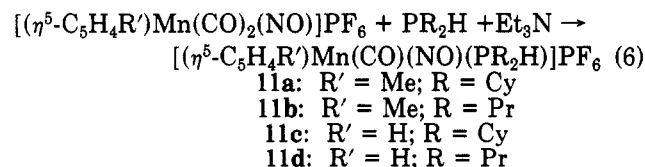
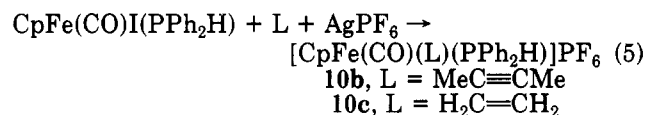
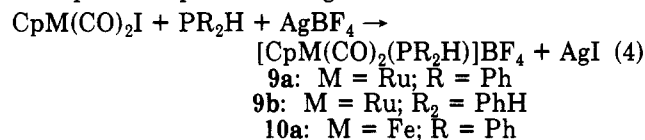
Subsequent formation of $[Cp(OC)_2M(\mu-PPh_2)(\mu-H)Pt(PPh_3)_2]^+$ involves protonation followed by CO displacement by PPh_3 . The protonation is M dependent, occurring at the metal-metal bond for 5 ($M = Mo$) to give $[Cp(OC)_2Mo(\mu-PPh_2)(\mu-H)Pt(CO)(PPh_3)]^+$, while for the tungsten analogue protonation occurs primarily at W to give $[Cp(OC)_2HW(\mu-PPh_2)Pt(CO)(PPh_3)]^+$ (existing in a dynamic equilibrium with a minor amount of $[Cp(OC)_2W(\mu-PPh_2)(\mu-H)Pt(CO)(PPh_3)]^+$). The cationic complexes $[CpRe(NO)(CO)(PR_2H)]BPh_4$ (6; $R = Cy, Ph, Pr$) react with $Pt(C_2H_4)(PPh_3)_2$ predominantly via route 1 to give $[Cp(OC)(ON)Re(\mu-PR_2)PtH(PPh_3)_2]^+$ (7) as relatively stable solution species (losing CO very slowly at 20 °C (days); eq 3).² Reaction with the more basic complex $Pt(PPh_3)_4$ proceeds predominantly via route 2 with rapid CO loss to give the μ -phosphido terminal rhenium hydride $[Cp(ON)HRe(\mu-PR_2)Pt(PPh_3)_2]^+$ (8; eq 3). This terminal rhenium hydride is the kinetic product of the reaction and undergoes an unusual Cl-catalyzed rearrangement to the thermodynamically preferred isomer $[Cp(ON)Re(\mu-$



$PR_2)(\mu-H)Pt(PPh_3)_2]^+$. The interconversion of terminal and bridged isomers may be slow (e.g. the RePt system²) or very fast (e.g. $[Cp(OC)_2W(H)(\mu-PPh_2)Pt(CO)PPh_3]^+$ ³ and $(OC)_3Fe(H)(\mu-PR_2)Pt(PPh_3)_2$,⁴ $\Delta G^\ddagger < 5$ kcal mol⁻¹, estimated from NMR studies). These previously reported studies¹⁻⁴ have established two reaction routes whereby the secondary phosphine complex $[M](CO)(PR_2H)^{n+}$ ($n = 0, 1$) can react with zerovalent platinum complexes to give the μ -hydrido compounds $[M](\mu-PR_2)(\mu-H)Pt(PR_3)_2$ as final products (Scheme I). We have extended these studies to other cationic secondary phosphine complexes and herein we report on the chemistry associated with the complexes $[CpM(CO)_2(PR_2H)]X$ (9a, $M = Ru, PR_2H = PPh_2H, X = BF_4$; 9b, $M = Ru, PR_2H = PPh_2H, X = BF_4$; 10a, $M = Fe, PR_2H = PPh_2H, X = PF_6$), $[CpFe(CO)(MeC\equiv CMe)(PPh_2H)]PF_6$ (10b), $[CpFe(CO)(C_2H_4)(PPh_2H)]PF_6$ (10c), $[(\eta^5-C_5H_4R')Mn(CO)(NO)(PR_2H)]PF_6$ (11a, $R' = Me, PR_2H = PCy_2H$; 11b, $R' = Me, PR_2H = PPr_2H$; 11c, $R' = H, PR_2H = PCy_2H$; 11d, $R' = H, PR_2H = PPr_2H$), and $[(\eta^7-C_7H_7)Mo(CO)_2(PCy_2H)]PF_6$ (12) and their reactions with Pt(0) complexes.

Results

Due to the high reactivity of P-H bonds, synthetic routes to generating $[M]PR_2H$ complexes usually require mild reaction conditions. The cationic secondary phosphine complexes 9-12 were prepared according to eq 4-7 by following procedures previously developed for the synthesis of tertiary phosphine complexes.⁶⁻⁸ Analytical and spectroscopic data are given in Table I.

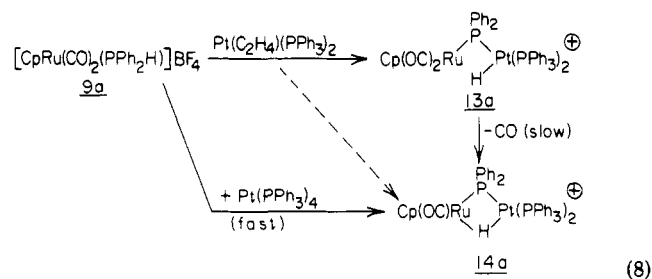


Reactions of $[CpM(CO)_2(PR_2H)]BF_4$ with Pt(0) Complexes. $[CpRu(CO)_2(PPh_2H)]BF_4$ (9a) reacts with $Pt(C_2H_4)(PPh_3)_2$ in CH_2Cl_2 to produce the cis terminal platinum hydride $[Cp(OC)_2Ru(\mu-PPh_2)PtH(PPh_3)_2]BF_4$ (13a) as the major product (Scheme I, route 1) together

(7) James, T. A.; McCleverty, J. A. *J. Chem. Soc. A* 1970, 850.

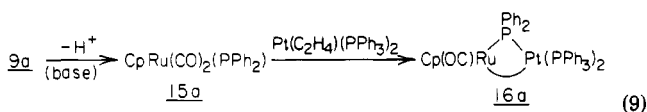
(8) Isaacs, E. E.; Graham, W. A. G. *J. Organomet. Chem.* 1975, 90, 319.

with a small amount of the hydrido-bridged $[\text{Cp}(\text{OC})\text{Ru}(\mu\text{-PPh}_2)(\mu\text{-H})\text{Pt}(\text{PPh}_3)_2]\text{BF}_4$ (**14a**; eq 8). Since the ter-

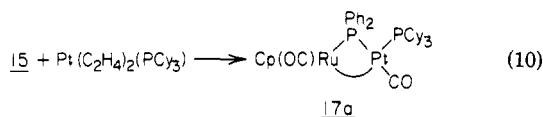


minal hydride **13a** loses CO to give the bridging hydride **14a** very slowly ($t_{1/2}$ for CO loss ca. 60 h at 20 °C), it is clear that **13a** is not an intermediate for the formation of the initially observed **14a**. A probable route to the initially produced **14a** is the deprotonation pathway (Scheme I, route 2). Consistent with this, the amount of **14a** formed on mixing $[\text{CpRu}(\text{CO})_2(\text{PPh}_2\text{H})]\text{BF}_4$ (**9a**) with $\text{Pt}(\text{C}_2\text{H}_4)(\text{PPh}_3)_2$ is *concentration dependent*, with dilute solutions resulting in the formation of **13a** only (IR monitoring of ν_{CO} region). A similar concentration effect has been noted and commented on for the reaction of $[\text{CpRe}(\text{CO})(\text{NO})(\text{PPh}_2\text{H})]\text{BF}_4$ with $\text{Pt}(\text{C}_2\text{H}_4)(\text{PPh}_3)_2$.² The reaction of $[\text{CpRu}(\text{CO})_2(\text{PPh}_2\text{H})]\text{BF}_4$ (**9a**) with the more basic complex $\text{Pt}(\text{PPh}_3)_4$ results in the *rapid* formation of the hydride-bridged $[\text{Cp}(\text{OC})\text{Ru}(\mu\text{-PPh}_2)(\mu\text{-H})\text{Pt}(\text{PPh}_3)_2]\text{BF}_4$ (**14a**) as the sole product (i.e. Scheme I, route 2). (Complex characterization is discussed later; spectroscopic data are given in Table II.)

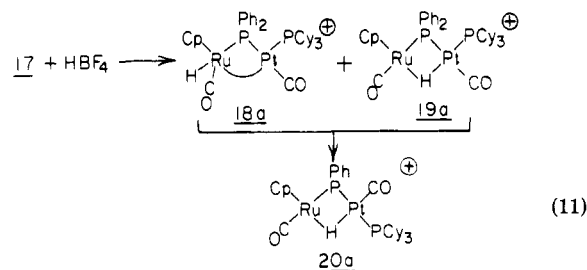
The complex $[\text{CpRu}(\text{CO})_2(\text{PPh}_2\text{H})]\text{BF}_4$ (**9a**) is readily deprotonated by Proton Sponge to give the very oxygen sensitive phosphido complex $\text{CpRu}(\text{CO})_2\text{PPh}_2$ (**15a**; prepared in situ). Reaction of **15a** with $\text{Pt}(\text{C}_2\text{H}_4)(\text{PPh}_3)_2$ in toluene gives the neutral bimetallic complex $\text{Cp}(\text{OC})\text{-Ru}(\mu\text{-PPh}_2)\text{Pt}(\text{PPh}_3)_2$ (**16a**; eq 9). This complex is



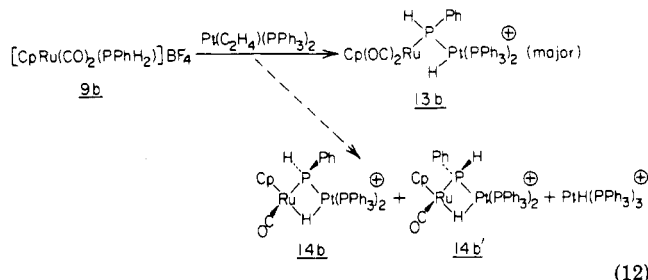
structurally similar to the previously reported $\text{Cp}(\text{OC})_2\text{M}(\mu\text{-PPh}_2)\text{Pt}(\text{PPh}_3)_2$ (**5**; M = Mo, W).³ Protonation of $\text{Cp}(\text{OC})\text{Ru}(\mu\text{-PPh}_2)\text{Pt}(\text{PPh}_3)_2$ (**16a**; HBF_4 in CH_2Cl_2) leads to the bridged hydrido cation **14a**. The reaction of $\text{CpRu}(\text{CO})_2\text{PPh}_2$ (**15a**) with $\text{Pt}(\text{C}_2\text{H}_4)_2(\text{PCy}_3)$ gives the neutral bimetallic complex $\text{Cp}(\text{OC})\text{Ru}(\mu\text{-PPh}_2)\text{Pt}(\text{CO})(\text{PCy}_3)$ (**17a**; eq 10). Protonation of **17a** with HBF_4 in



CD_2Cl_2 (NMR monitoring) gives initially an equilibrium mixture of the isomeric terminal hydrido cation $[\text{Cp}(\text{OC})(\text{H})\text{Ru}(\mu\text{-PPh}_2)\text{Pt}(\text{CO})(\text{PCy}_3)]^+$ (**18a**) and the hydrido-bridged cation $[\text{Cp}(\text{OC})\text{Ru}(\mu\text{-PPh}_2)(\mu\text{-H})\text{Pt}(\text{CO})(\text{PCy}_3)]^+$ (**19a**). These slowly rearrange (ca. 10 h, 20 °C) to the hydrido-bridged cation **20** (eq 11). The primary phosphine complex $[\text{CpRu}(\text{CO})_2(\text{PPh}_2\text{H})]\text{BF}_4$ (**9b**) reacts with $\text{Pt}(\text{C}_2\text{H}_4)(\text{PPh}_3)_2$ to give *mainly* the terminal hydride $[\text{Cp}(\text{OC})_2\text{Ru}(\mu\text{-PhH})\text{PtH}(\text{PPh}_3)_2]^+$ (cation of **13b**; Scheme I, route 1) together with small amounts of $[\text{PtH}(\text{PPh}_3)_3]^{+9}$



and the diastereotopic hydrido-bridged isomers $[\text{Cp}(\text{OC})\text{Ru}(\mu\text{-PPhH})(\mu\text{-H})\text{Pt}(\text{PPh}_3)_2]^+$ (cation of **14b** and **14b'**; Scheme I, route 2; eq 12). The ratio of **14b** to **14b'**



is ca. 1:1. The *cis* terminal hydride **13b** is rather inert to CO loss. Conversion of the terminal hydride **13b** to the bridged hydrides **14b** and **14b'** required ca. 40 h of reflux in THF with **14b** and **14b'** being formed in a ca. 2:1 ratio. (Which is the major isomer is not known, though on steric grounds **14b'** may be the preferred isomer.) The reaction of $[\text{CpRu}(\text{CO})_2(\text{PPh}_2\text{H})]\text{BF}_4$ (**9b**) with $\text{Pt}(\text{PPh}_3)_4$ surprisingly gave mainly the *cis* terminal Pt hydride **13b**, in contrast to the case for **9a**, which reacts with $\text{Pt}(\text{PPh}_3)_4$ to give mainly the hydrido-bridged cation **14a**.

The reactions of $[\text{CpFe}(\text{CO})_2(\text{PPh}_2\text{H})]\text{PF}_6$ (**10a**) with $\text{Pt}(\text{C}_2\text{H}_4)(\text{PPh}_3)_2$ and $\text{Pt}(\text{PPh}_3)_4$ are very similar to those of the ruthenium analogue **9a**. Noticeable differences are as follows: (i) the conversion of $[\text{Cp}(\text{OC})_2\text{Fe}(\mu\text{-PPh}_2)\text{PtH}(\text{PPh}_3)_2]\text{PF}_6$ (**21**) to $[\text{Cp}(\text{OC})\text{Fe}(\mu\text{-PPh}_2)(\mu\text{-H})\text{Pt}(\text{PPh}_3)_2]\text{PF}_6$ (**22**; CO loss complete within 2 h) is faster than for the ruthenium system (**13a** \rightarrow **14a**; eq 8); (ii) a considerable amount of $[\text{PtH}(\text{PPh}_3)_3]\text{PF}_6$ is formed; (iii) attempts to isolate neutral FePt bimetallics structurally similar to

$\text{Cp}(\text{OC})\text{Ru}(\mu\text{-PPh}_2)\text{Pt}(\text{PPh}_3)_2$ (**16a**) were not successful. The structurally similar $[\text{CpFe}(\text{CO})(\text{MeC}\equiv\text{CMe})(\text{PPh}_2\text{H})]\text{PF}_6$ (**10b**) reacted with $\text{Pt}(\text{C}_2\text{H}_4)(\text{PPh}_3)_2$ to give $[\text{Cp}(\text{OC})\text{Fe}(\mu\text{-PPh}_2)(\mu\text{-H})\text{Pt}(\text{PPh}_3)_2]\text{PF}_6$ (**22**) as the major product (reaction complete within 20 min). In preparative reactions $[\text{Cp}(\text{OC})\text{Fe}(\mu\text{-PPh}_2)(\mu\text{-H})\text{Pt}(\text{PPh}_3)_2]\text{PF}_6$ (**22**) was more easily isolated from **10b** than from **10a**. The ethylene-containing $[\text{CpFe}(\text{CO})(\text{C}_2\text{H}_4)(\text{PPh}_2\text{H})]\text{PF}_6$ (**10c**) reacted with $\text{Pt}(\text{C}_2\text{H}_4)(\text{PPh}_3)_2$ to give $[\text{Cp}(\text{OC})(\text{C}_2\text{H}_4)\text{Fe}(\mu\text{-PPh}_2)\text{PtH}(\text{PPh}_3)_2]\text{PF}_6$ (**23**) as a relatively long-lived solution species that, over a period of ca. 3 h, lost C_2H_4 to give **22**. These observations raise the *possibility* of acetylene and ethylene transfer from Fe to Pt via but-2-yne or C_2H_4 bridging structures. (N.B. While C_2H_4 is not a good bridging ligand, it should be noted that an intramolecular transfer of a PPh_3 ligand (likely not a good bridge ligand) between adjacent Pt atoms has been recently observed in the complex $[\text{Pt}_3(\text{CO})(\text{PPh}_3)(\text{dppm})_3]^{2+}$.¹⁰) The reaction of $[\text{CpFe}(\text{CO})_2(\text{PPh}_2\text{H})]\text{PF}_6$ with $\text{Pt}(\text{C}_2\text{H}_4)_2(\text{PCy}_3)$ gave the complex $[\text{Cp}(\text{OC})\text{Fe}(\mu\text{-PPh}_2)(\mu\text{-H})\text{Pt}(\text{CO})(\text{PCy}_3)]\text{PF}_6$ (**24**), structurally analogous to **20a** (eq 11).

(9) Dingle, T. W.; Dixon, K. *Inorg. Chem.* 1974, 13, 847.

(10) Bradford, A. M.; Jennings, M. C.; Puddephatt, R. J. *Organometallics* 1988, 7, 792.

from neutral to positively charged systems could well reflect the lower trans effect of the hydrido ligand in a PtHP_3^+ system vis à vis that in a neutral PtHP_3 system¹⁸ and, hence, an increased ΔG^\ddagger for substitution of PPh_3 trans to H in the formation of $[\text{M}(\mu\text{-PR}_2)(\mu\text{-CO})\text{PtH}(\text{PPh}_3)]^+$. Besides CO labilization the mechanistic features of Scheme I, route 1, also allow for halide,¹⁹ carbene,²⁰ probably acetylene, and possibly olefin transfer from 18-electron metal centers to an adjacent 16-electron Pt center. Features favoring the initial protonation pathway (Scheme I, route 2) are acidic P-H bonds and basic Pt(0) complexes. Consequently, this route is more probable for cationic systems and for PPh_2H complexes vs PCy_2H or *P-n-Pr*₂H complexes and is facilitated by the presence of proton bases (e.g. Proton Sponge) and basic Pt complexes ($\text{Pt}(\text{PPh}_3)_4 > \text{Pt}(\text{C}_2\text{H}_4)(\text{PPh}_3)_2$).

Correlation of $^1J_{195\text{Pt}-1\text{H}}$, $^1J_{195\text{Pt}-3\text{IP}}$, and $^2J_{31\text{P}-3\text{IP}}$ Data for Systems of the Type $[\text{M}](\mu\text{-PPh}_2)(\mu\text{-H})\text{Pt}(\text{PPh}_3)_2$. The possibility of a correlation between $^1J_{195\text{Pt}-3\text{IP}}$ data and Pt-P bond distances in Pt^{II} -phosphine complexes has been the subject of several investigations.^{21,22} While both parameters are expected to be sensitive to s orbital character of the bond, several molecular variables contribute to the magnitude of $^1J_{195\text{Pt}-3\text{IP}}$ ²³ and the correlations are, in the main, rather poor. In contrast we have recently observed a good correlation for $^1J_{195\text{Pt}-3\text{IP}}$ /P-Pt bond length data for the PtP_3 fragment in the closely related cations $[\text{Cp}(\text{ON})\text{Re}(\mu\text{-PR}_2)(\mu\text{-H})\text{Pt}(\text{PPh}_3)_2]^+$ (R = Ph, Cy) and $[\text{Cp}(\text{ON})\text{HRe}(\mu\text{-PCy}_2)\text{Pt}(\text{PPh}_3)_2]^+$.² Particularly noteworthy were the observations that the $\text{P}_\mu\text{-Pt}$ bond lengths were significantly shorter than Pt-PPh₃ bond lengths in comparable coordination sites and that for the same bond length $^1J_{195\text{Pt}-3\text{IP}}$ is less than 50% of the value for $^1J_{195\text{Pt}-3\text{IPPh}_3}$. This suggested a lower phosphorus s orbital contribution to the $\text{P}_\mu\text{-Pt}$ bond, possibly reflective of ring strain effects (N.B. $\text{Re-P}_\mu\text{-Pt} \approx 77^\circ$). Consistent with this argument is the decrease in the trans $^2J_{31\text{P}-3\text{IP}}$ coupling from ca. 325 Hz in $[\text{Cp}(\text{OC})_2\text{Ru}(\mu\text{-PR}_2)\text{PtH}(\text{PPh}_3)_2]\text{BF}_4$ (13) to ca. 230 Hz in $[\text{Cp}(\text{OC})\text{Ru}(\mu\text{-PR}_2)(\mu\text{-H})\text{Pt}(\text{PPh}_3)_2]\text{BF}_4$ (14). With respect to ring strain arguments it is interesting to note that $^1J_{31\text{P}-1\text{H}}$ for the $\mu\text{-PPhH}$ ligand increases from 334 Hz in $[\text{Cp}(\text{OC})_2\text{Ru}(\mu\text{-PPhH})\text{PtH}(\text{PPh}_3)_2]\text{BF}_4$ (13b) to 392 Hz in $[\text{Cp}(\text{OC})_2\text{Ru}(\mu\text{-PPhH})(\mu\text{-H})\text{Pt}(\text{PPh}_3)_2]\text{BF}_4$ (14b), suggestive of an increase in s character in the P-H bond in the ring-strained structure 14b. Similar, though smaller, changes in $^1J_{31\text{P}-1\text{H}}$ for the hypophosphite anion H_2PO_2^- in the presence of added cations have been interpreted in terms of increases in $^1J_{31\text{P}-1\text{H}}$ being linked with $\text{H}_2\text{PO}_2^- \text{M}^+$ association and a decrease in O-P-O upon chelation of M^+ by the anion.²⁴

We have explored possible correlations involving coupling constant data for a range of structurally similar complexes containing the $[\text{M}](\mu\text{-PPh}_2)(\mu\text{-H})\text{Pt}(\text{PPh}_3)_2$ unit (Figure 1). For these systems the basic coordination unit at Pt is essentially constant, only small variations associated with changes in [M] are being studied, and coupling constant data are available for all four donor atom-Pt interactions (not the case in previous studies). In Figure

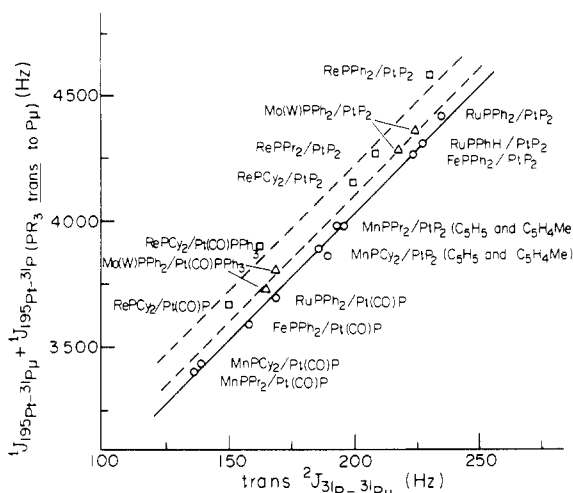


Figure 2. Plot of $\sum ^1J_{195\text{Pt}-3\text{IP}}$ for P_μ and the PR_3 ligand trans to P_μ vs the trans $^2J_{31\text{P}-31\text{P}}$ coupling constant for the structurally similar cations $[\text{M}](\mu\text{-PR}_2)(\mu\text{-H})\text{Pt}(\text{PPh}_3)_2^+$ (PtP_2 systems) and $[\text{M}](\mu\text{-PR}_2)(\mu\text{-H})\text{Pt}(\text{CO})(\text{PCy}_3)^+$ ($\text{Pt}(\text{CO})\text{P}$ systems): (O) $[\text{M}] = [\text{Cp}(\text{CO})\text{M}]$ ($\text{M} = \text{Fe}, \text{Ru}$), $[\text{Cp}(\text{NO})\text{Mn}]$; (□) $[\text{M}] = [\text{Cp}(\text{NO})\text{Re}]$; (Δ) $[\text{M}] = [\text{Cp}(\text{CO})_2\text{M}]$ ($\text{M} = \text{Mo}, \text{W}$). Labeling of points is according to the MPR_2/Pt system.

1, individual and average values of all three $^1J_{195\text{Pt}-3\text{IP}}$ couplings for a series of $[\text{M}](\mu\text{-PPh}_2)(\mu\text{-H})\text{Pt}(\text{PPh}_3)_2$ systems are plotted against the one-bond coupling constant to the fourth ligand, $^1J_{195\text{Pt}-1\text{H}}$ (hydride). In mononuclear Pt(II) hydrides, changes in $^1J_{195\text{Pt}-1\text{H}}$ correlate mainly with changes in the trans ligand (NMR trans influence¹⁸). In contrast, in the bimetallic systems (Figure 1) (i) all three $^1J_{195\text{Pt}-3\text{IP}}$ couplings vary considerably as $^1J_{195\text{Pt}-1\text{H}}$ varies, (ii) $^1J_{195\text{Pt}-3\text{IP}}$ (cis to H) exhibits the largest percentage variation, and (iii) while the correlation of $^1J_{195\text{Pt}-3\text{IP}}$ with $^1J_{195\text{Pt}-1\text{H}}$ is rather poor for individual coupling constants, a much improved result is obtained when the average of all three $^1J_{195\text{Pt}-3\text{IP}}$ values is used. These observations suggest that individual Pt-P bonds are easily distorted but that there is an internal self-compensating effect such that the net effect, as measured/reflected by the average $^1J_{195\text{Pt}-3\text{IP}}$ value, correlates well with changes in the Pt-H bond as measured/reflected by $^1J_{195\text{Pt}-1\text{H}}$. We have recently shown that distortions in Pt(II) phosphine complexes, as reflected by P-Pt-P bond angle data, can be successfully rationalized in terms of P-Pt bond bending²⁵ and suggest that similar distortions may contribute to the relatively poor correlations for individual $^1J_{195\text{Pt}-3\text{IP}}$ values (Figure 1). Particularly noticeable is the sensitivity of $^1J_{195\text{Pt}-3\text{IP}}$ and $^2J_{31\text{P}-31\text{P}}$ to changes in [M] or changes in ligands on Pt. The sensitivity of $^1J_{195\text{Pt}-3\text{IP}}$ to changes in [M] and to replacement of the PPh_3 trans to H by a CO ligand is considerably greater in both absolute and percentage terms when compared to the effect of these changes on $^1J_{195\text{Pt}-3\text{IP}}$ for the PR_3 ligand trans to P_μ (see Table II). The decrease in $^1J_{195\text{Pt}-3\text{IP}}$ on replacing the PPh_3 (cis to P_μ) with CO is also reflected in the $^2J_{31\text{P}-31\text{P}}$ couplings to PR_3 trans to P_μ , which decrease markedly from ca. 200–235 to 140–170 Hz. Figure 2 is a plot of $^2J_{31\text{P}-31\text{P}}(\text{trans})$ vs $\sum [^1J_{195\text{Pt}-3\text{IP}} + ^1J_{195\text{Pt}-3\text{IP}\mu}]$ for a range of structurally similar complexes containing the $\text{trans-}[\text{M}](\mu\text{-PR}_2)(\mu\text{-H})\text{PtL}(\text{PR}_3)$ unit. A reasonably linear correlation is observed for a range of Fe, Mn, and Ru complexes with slight variation for Re and Mo/W systems. This correlation is understandable if the major variation is to be found in the P_μ s-orbital contribution to the $\text{P}_\mu\text{-Pt}$ bond.

(18) Appleton, T. G.; Clark, H. C.; Manzer, L. E. *Coord. Chem. Rev.* 1973, 10, 335.

(19) Powell, J.; Tucks, E. Unpublished results.

(20) Powell, J.; Fuchs, E.; Sawyer, J. F. *Manuscript in preparation.*

(21) Bao, Q.-B.; Geib, S. J.; Rheingold, A. L.; Brill, T. B. *Inorg. Chem.* 1987, 26, 3453.

(22) Mather, G. G.; Pidcock, A.; Rapsey, G. J. *N. J. Chem. Soc., Dalton Trans.* 1973, 2095.

(23) Pople, J. A.; Santry, D. P. *Mol. Phys.* 1964, 8, 1.

(24) Spitz, F. R.; Cabral, J.; Haake, P. *J. Am. Chem. Soc.* 1986, 108, 2802.

(25) Powell, J. *J. Chem. Soc., Chem. Commun.* 1989, 200.

Experimental Section

General Considerations. All manipulations were carried out under an atmosphere of dry N_2 or argon, with use of dry and degassed solvents. IR spectra (CH_2Cl_2 solution) were recorded on a Nicolet 10DX spectrometer. 1H and $^{31}P\{^1H\}$ NMR spectra (CD_2Cl_2 solution) were obtained on a Varian XL200 spectrometer, and chemical shifts were referenced to tetramethylsilane and 85% H_3PO_4 , respectively. Microanalyses were carried out by Canadian Microanalytical Laboratories of Vancouver, Canada.

Starting Materials. $[CpRu(CO)_2I]$,²⁶ $[CpFe(CO)_2I]$,²⁷ $[(\eta^5-C_5H_4R')Mn(CO)_2(NO)]PF_6$ ($R' = CH_3, H$),²⁸ $[(\eta^7-C_7H_7)Mo(CO)_3]PF_6$,²⁹ $Pt(C_2H_4)(PPh_3)_2$,³⁰ and $Pt(C_2H_4)_2(PCy_3)_2$ ³¹ were prepared by following the appropriate literature procedure. PPh_2H , PPh_2H_2 , and PCy_2H were purchased from either Pressure Chemical Co. or Strem Chemical Inc.

$[CpRu(CO)_2(PPh_2H)]BF_4$ (9a). $AgBF_4$ (0.514 g) was added to a solution of $CpRu(CO)_2I$ (0.412 g, 1.18 mmol) and PPh_2H (0.25 mL) in CH_2Cl_2 (10 mL) and the reaction mixture stirred overnight. The reaction mixture was checked for completion by IR spectroscopy. (If $CpRu(CO)_2I$ was still present, more $AgBF_4$ was added and the reaction mixture stirred for several more hours.) The reaction mixture was filtered through Celite several times and pumped to dryness and the residue recrystallized three times from CH_2Cl_2 /diethyl ether to give **9a** as a white crystalline product (35% yield). A similar procedure gave **9b** (30% yield). The low yields were due to the difficulty of obtaining the complexes free of $AgBF_4$ contamination.

$[CpFe(CO)_2(PPh_2H)]PF_6$ (10a) was prepared (50% yield) with use of $AgPF_6$, and by a similar procedure $[CpFe(CO)(MeC\equiv CMe)(PPh_2H)]PF_6$ and $CpFe(CO)(C_2H_4)(PPh_2H)]PF_6$ (**10c**) were prepared (ca. 40% yield) from $CpFeI(CO)(PPh_2H)$, $AgPF_6$, and either $MeC\equiv CMe$ or $H_2C=CH_2$ by following the method of Reger et al.⁶ for the synthesis of $[CpFe(CO)(MeC\equiv CMe)(PPh_3)]PF_6$ and $[CpFe(CO)(C_2H_4)(PPh_3)]PF_6$.

$[(\eta^5-C_5H_4Me)Mn(CO)(NO)(PCy_2H)]PF_6$ (11a). Et_3N (~0.2 mL) was added to a solution of $[(\eta^5-C_5H_4Me)Mn(CO)_2(NO)]PF_6$ (1.02 g) and PCy_2H (0.70 mL) in acetone (30 mL). The reaction mixture was stirred for 30 min, ethanol (70 mL) added, and the volume reduced under vacuum to 35 mL. When the mixture was cooled, **11a** was obtained as orange crystals (60% yield). Complexes **11b-d** were similarly prepared in 40–60% yields.

$[(\eta^7-C_7H_7)Mo(CO)_2(PCy_2H)]PF_6$ (12). To a suspension of $[(\eta^7-C_7H_7)Mo(CO)_3]PF_6$ (1.49 g) in 95% ethanol (150 mL) at 50 °C was slowly added a solution of PCy_2H (0.80 mL, 1.02 equiv) in 95% ethanol (60 mL) (addition time 1–2 h). The reaction mixture was cooled and left in the freezer overnight. Filtration of the resultant orange crystals gave **12** (57% yield).

$[Cp(OC)Ru(\mu-PPh_2)(\mu-H)Pt(PPh_3)_2]BF_4$ (14a). $[CpRu(CO)_2(PPh_2H)]BF_4$ (0.202 g) and $Pt(C_2H_4)(PPh_3)_2$ (0.325 g) were

refluxed in THF for 3 h. When the solution was cooled and the volume reduced under vacuum, **14a** precipitated as a bright yellow powder (0.416 g, 85% yield). Anal. Calcd (found) for $C_{54}H_{46}BF_4OP_3PtRu$: C, 54.64 (54.42); H, 3.88 (3.66).

$[Cp(OC)Fe(\mu-PPh_2)(\mu-H)Pt(PPh_3)BF_4]$ (22). $Pt(C_2H_4)(PPh_3)_2$ (0.311 g) was added to a CH_2Cl_2 solution (3 mL) of $[CpFe(CO)(MeC\equiv CMe)(PPh_2H)]BF_4$ (0.197 g). After the mixture stood at room temperature for 1 h, a few drops of pentane were added to precipitate trace amounts of $CpFeCl(CO)(PPh_3)$ as green crystals. After filtration, diethyl ether (2 mL) was added to the filtrate and the solution cooled to -20 °C. The complex **22** slowly crystallized as red prisms (0.180 g, 38%). Anal. Calcd (found) for $C_{54}H_{46}BF_4FeOP_3Pt$: C, 56.84 (56.31); H, 4.03 (4.06).

$[Cp(OC)Fe(\mu-PPh_2)(\mu-H)Pt(CO)(PCy_3)]PF_6$ (24). $Pt(C_2H_4)_2(PCy_3)_2$ (0.203 g) was added to a CH_2Cl_2 solution (2 mL) of $[CpFe(CO)_2(PPh_2H)]PF_6$ (0.194 g). After 3 h addition of hexane (5 mL) precipitated **24** as a red-purple powder (0.306 g, 80% yield). Anal. Calcd (found) for $C_{37}H_{49}F_6FeO_2P_3Pt$: C, 45.21 (45.71); H, 4.98 (5.41).

$[(\eta^5-C_5H_4Me)(ON)Mn(\mu-P-n-Pr_2)(\mu-H)Pt(PPh_3)_2]PF_6$ (25). $Pt(C_2H_4)(PPh_3)_2$ (0.224 g) was added to $[(\eta^5-C_5H_4Me)Mn(CO)(NO)(P-n-Pr_2H)]PF_6$ (0.128 g) in CH_2Cl_2 (15 mL) and the solution allowed to stand overnight. The volume was reduced under vacuum, hexane added, and the solution cooled to -20 °C. The complex **25** was obtained as purple air-sensitive crystals (0.215 g, 67% yield). Anal. Calcd (found) for $C_{48}H_{52}F_6MnNOP_4Pt$: C, 50.26 (49.85); H, 4.54 (4.21); N, 1.22 (1.10).

$[(\eta^7-C_7H_7)(OC)Mo(\mu-PCy_2)(\mu-H)Pt(PPh_3)_2]PF_6$ (27). $[(\eta^7-C_7H_7)Mo(CO)_2(PCy_2H)]PF_6$ (0.158 g) and $Pt(C_2H_4)(PPh_3)_2$ (0.403 g, 2 equiv) were stirred in CH_2Cl_2 (15 mL) for 15 min, at which stage solution IR spectroscopy (ν_{CO} region) indicated that all the starting Mo complex had gone and that $[(\eta^7-C_7H_7)(OC)Mo(\mu-PCy_2)(\mu-H)Pt(CO)(PPh_3)]PF_6$ and $Pt(PPh_3)_2$ were the major solution species. Triphenylphosphine (0.080 g, 1.1 equiv) was added and the solution stirred for a further 30 min. Removal of the solvent gave a yellow-green residue, which after several recrystallizations from CH_2Cl_2 /hexane gave **27** as a yellow powder (0.125 g, 36% yield). Anal. Calcd (found) for $C_{56}H_{60}F_6MoOP_4Pt$: C, 52.60 (52.24); H, 4.73 (4.42).

$[(\eta^7-C_7H_7)(OC)Mo(\mu-PCy_2)(\mu-H)Pt(CO)(PCy_3)]PF_6$ (26b). $[(\eta^7-C_7H_7)Mo(CO)_2(PCy_2H)]PF_6$ (0.120 g) and $Pt(C_2H_4)_2(PCy_3)_2$ (0.110 g, 1.02 equiv) were stirred in CH_2Cl_2 (20 mL) for 5 h. The solvent was removed (vacuum) and the residue recrystallized from CH_2Cl_2 /hexane to give green crystals of **26b** (0.132 g, 65% yield). Anal. Calcd (found) for $C_{39}H_{63}F_6MoO_2P_3Pt$: C, 44.11 (43.02); H, 5.98 (5.82).

The other MPt bimetallic complexes described in this paper were characterized spectroscopically (Tables I and II). The complex $Cp(OC)Ru(\mu-PPh_2)Pt(PPh_3)_2$ (**16a**) could be precipitated from CH_2Cl_2 solution by the addition of hexane as an orange air-sensitive solid. Attempts to recrystallize **16a** for elemental analysis resulted in considerable decomposition and were not successful. **16a** is structurally similar to the more stable complex $Cp(OC)_2W(\mu-PPh_2)Pt(PPh_3)_2$.³

Acknowledgment. We thank the Natural Science and Engineering Research Council of Canada for financial support.

(26) Blackmore, T.; Cotton, J. D.; Bruce, M. I.; Stone, F. G. A. *J. Chem. Soc. A* 1968, 2931.

(27) Piper, T. S.; Wilkinson, G. *J. Inorg. Nucl. Chem.* 1956, 2, 38.

(28) *Organometallic Chemistry*; Eisch, J. J., King, R. B., Eds.; Academic Press: New York, 1965; Vol. 1, p 63.

(29) King, R. B. *Transition-Metal Compounds. Organometallic Synthesis*; Academic Press: London, 1965; Vol. 1, p 125.

(30) Blake, D. M.; Roundhill, D. M. *Inorg. Synth.* 1978, 18, 120.

(31) Spencer, J. L. *Inorg. Synth.* 1979, 19, 216.